A low-cost benthic incubation chamber for in-situ community metabolism measurements

Jennifer Mallon [Corresp., 1] , Anastazia T Banaszak [2] , Lauren Donachie [3] , Dan Exton [3] , Tyler Cyronak [4] , Thorsten Balke [1] , Adrian Bass [1]

[1] School of Geographical and Earth Sciences, University of Glasgow, Glasgow, United Kingdom

[2] Unidad Académica de Sistemas Arrecifales, Universidad Nacional Autónoma de México, Puerto Morelos, Quintana Roo, Mexico

[3] Operation Wallacea, Spilsby, Lincolnshire, United Kingdom

[4] Department of Marine and Environmental Sciences, Halmos College of Natural Sciences and Oceanography, Nova Southeastern University, Dania Beach, Florida, United States

Corresponding Author: Jennifer Mallon
Email address: j.mallon.1@research.gla.ac.uk

Benthic incubation chambers facilitate in-situ metabolism studies in shallow water environments. They are used to isolate the water surrounding a study organism or community so that changes in water chemistry can be quantified to characterise physiological processes such as photosynthesis, respiration, and calcification. Such field measurements capture the biological processes taking place within the benthic community while incorporating the influence of environmental variables that are often difficult to recreate in ex-situ settings. Variations in benthic chamber designs have evolved for a range of applications. In this study, we built upon current designs to create a novel chamber, which is (1) low-cost and assembled without specialised equipment, (2) easily reproducible, (3) minimally invasive, (4) adaptable to varied substrates, and (5) comparable with other available designs in performance. We tested the design in the laboratory and field and found that it achieved the outlined objectives. Using non-specialised materials, we were able to construct the chamber at a low cost (under $20 USD per unit), while maintaining similar performance and reproducibility with that of existing designs. Laboratory and field tests demonstrated minimal leakage (2.08 ± 0.78 % water exchange over 4 hours) and acceptable light transmission (86.9 ± 1.9 %), results comparable to those reported for other chambers. In the field, chambers were deployed in a shallow coastal environment in Akumal, Mexico, to measure productivity of (a) seagrass, and (b) coral-, algae-, and sand-dominated reef patches. In both case studies, production rates aligned with those of comparable benthic chamber deployments in the literature and followed established trends with light, the primary driver of benthic metabolism, indicating robust performance under field conditions. We demonstrate that our low-cost benthic chamber design uses locally accessible and minimal resources, is adaptable for a variety of

field settings, and can be used to collect reliable and repeatable benthic metabolism data. This chamber has the potential to broaden accessibility and applications of in-situ incubations for future studies.

1   **A low-cost benthic incubation chamber for in-situ community metabolism measurements**

2   Jennifer Mallon[1]; Anastazia T Banaszak[2]; Lauren H Donachie[3]; Dan A Exton[3]; Tyler Cyronak[4];

3   Thorsten Balke[1]; Adrian Bass[1]

4   [1]School of Geographical and Earth Sciences, University of Glasgow, Glasgow, Scotland

5   [2]Unidad Académica de Sistemas Arrecifales, Universidad Nacional Autónoma de México,

6   Puerto Morelos, Mexico

7   [3]Operation Wallacea, Spilsby, Lincolnshire, United Kingdom

8   [4]Department of Marine and Environmental Sciences, Halmos College of Natural Sciences and

9   Oceanography**,** Nova Southeastern University, Dania Beach, Florida, USA

10   Corresponding author: Jennifer Mallon, East Quadrangle, Geographical and Earth Sciences,

11   University of Glasgow, University Avenue, Glasgow, G12 8QQ, Scotland.

12   **Abstract**

13   Benthic incubation chambers facilitate in-situ metabolism studies in shallow water environments.

14   They are used to isolate the water surrounding a study organism or community so that changes in

15   water chemistry can be quantified to characterise physiological processes such as photosynthesis,

16   respiration, and calcification. Such field measurements capture the biological processes taking

17   place within the benthic community while incorporating the influence of environmental variables

18   that are often difficult to recreate in ex-situ settings. Variations in benthic chamber designs have

19   evolved for a range of applications. In this study, we built upon current designs to create a novel

20   chamber, which is (1) low-cost and assembled without specialised equipment, (2) easily

21   reproducible, (3) minimally invasive, (4) adaptable to varied substrates, and (5) comparable with

22   other available designs in performance. We tested the design in the laboratory and field and

23   found that it achieved the outlined objectives. Using non-specialised materials, we were able to

24   construct the chamber at a low cost (under \$20 USD per unit), while maintaining similar

25   performance and reproducibility with that of existing designs. Laboratory and field tests

26   demonstrated minimal leakage (2.08 ± 0.78 % water exchange over 4 hours) and acceptable light

27   transmission (86.9 ± 1.9 %), results comparable to those reported for other chambers. In the

28   field, chambers were deployed in a shallow coastal environment in Akumal, Mexico, to measure

29   productivity of (a) seagrass, and (b) coral-, algae-, and sand-dominated reef patches. In both case

30   studies, production rates aligned with those of comparable benthic chamber deployments in the

31   literature and followed established trends with light, the primary driver of benthic metabolism,

32   indicating robust performance under field conditions. We demonstrate that our low-cost benthic

33   chamber design uses locally accessible and minimal resources, is adaptable for a variety of field

34   settings, and can be used to collect reliable and repeatable benthic metabolism data. This

35 chamber has the potential to broaden accessibility and applications of in-situ incubations for

36 future studies.

37 **Introduction**

38 Quantifying the relative balance of autotrophic and heterotrophic processes taking place within a

39 benthic community provides insight into ecosystem functioning and species composition

40 (Albright et al. 2015; Cyronak et al. 2018). As coastal ecosystems undergo degradation,

41 understanding ecosystem capacity for oxygen production and carbon cycling through

42 photosynthesis is critical. For example, defining ecosystem productivity can support

43 conservation of high 'blue carbon value' ecosystems (Duarte et al. 2010, 2013) and

44 characterisation of community metabolism facilitates geographical and temporal comparisons of

45 ecological function, which otherwise might be logistically limited (Cyronak et al. 2018; Lange et

46 al. 2020). Measurements of in-situ community metabolism capture individual rates of

47 productivity for functional groups and species, as well as the interactive physiological processes

48 taking place within the entire benthic community, rather than the simplified, reconstructed

49 communities often used in ex-situ measurements. Such measures offer important insight into the

50 critical role of coastal marine ecosystems for carbon capture and cycling.

51 Rates of photosynthesis and respiration can be measured directly from fluxes in dissolved

52 oxygen concentrations to calculate the net community productivity (NCP) taking place within a

53 benthic community. The development of in-situ gear to incubate benthic organisms and

54 communities has been guided by distinct research applications. Ecosystem metabolism can be

55 measured via three main approaches in the field; benthic boundary layer and eddy covariance

56 (e.g., Long et al. 2015; Takeshita et al. 2016; Berg et al. 2019), flow respirometry using

57 Lagrangian and Eularian adaptations (e.g., Barnes 1983; Falter et al. 2008; Shaw et al. 2014),

58   and enclosed incubations (see examples in Table 1). This study focusses on the incubation

59   method as a straightforward approach for deriving metabolic rates of single organisms or benthic

60   communities in the field.

61   Benthic chambers can be deployed in the field to contain sediments, corals, seagrasses, and other

62   biota, either as communities or as individual organisms, for periods of hours to days to capture

63   in-situ measurements of community or organismal metabolic rates (e.g. Huettel and Gust 1992;

64   Yates and Halley 2003; Wild et al. 2005; Murphy et al. 2012; Camp et al. 2015; van Heuven et

65   al. 2018; Roth et al. 2019). Standard benthic chamber designs consist of a tent or dome made

66   from a rigid, transparent container with a circulation pump (to mimic natural water flow), and a

67   sampling port (e.g., Roth et al., 2019, Table 1). Some chambers can only be deployed in areas

68   where substrate is suitable for the chamber base to be inserted, for example, often the base must

69   be buried in sand or sediments to create an effective seal (e.g., Olivé et al. 2016). However, the

70   technology has evolved to encompass a range of applications from smaller, single organism

71   chambers to larger community enclosures (Table 1). For example, high precision, real-time, in-

72   situ metabolism measurements of small surface areas of coral have been made possible by the

73   development of a high-tech adaptation of the benthic chamber concept: the Coral In Situ

74   Metabolism and Energetics (CISME) system, described in Murphy et al. (2012). CISME is a

75   specialised underwater respirometer that incubates small areas (~ 24.5 cm^2) of live coral to

76   measure pH, dissolved oxygen, and temperature changes. The electronic housing has waterproof

77   cables supplying power, a recirculation pump, and LED control, while a water sample loop holds

78   incubation samples so that total alkalinity can be used to derive calcification rates.

79   At the opposite end of the size-spectrum, large tent-like structures have been developed to

80   incubate entire patches of benthic communities (surface areas of several m^2). For example, the

81   Submersible Habitat for Analysing Reef Quality (SHARQ) developed by Yates and Halley

82   (2003) and other large tent enclosures such as the one described by van Heuven et al. (2018),

83   allow for measurements of seawater chemistry and can even be adapted for in-situ experiments

84   adding CO_2 or other treatments, e.g., Kline et al. (2012). The SHARQ and similar chamber

85   designs (e.g., van Heuven et al. 2018) incorporate a submersible circulation pump to ensure

86   turbulent flow within the incubated area. Flow is a primary driver of benthic metabolism and

87   regulates organism response to environmental effects such as ocean acidification (Comeau et al.

88   2014, 2019). The costs of building such chambers are moderate to high, and multiple replicate

89   chambers for parallel incubations further raise the costs, while specialised materials may be

90   difficult to source in some parts of the world where coral reefs and seagrasses are most abundant.

91   Submersible pumps, bespoke parts, and other expensive materials create an economic barrier to

92   the in-situ incubation chamber technique. To address these limitations, the Flexi-chamber,

93   developed by Camp et al. (2015), requires minimal specialised materials and can be constructed

94   at a low cost (< USD $20). The Flexi-chamber is made of a flexible plastic bag with a sampling

95   valve installed, which is attached to the base of the study organism with a cable tie. Both the bag

96   and valve were sourced from a medical supply store. The Flexi-chamber can be used to measure

97   metabolism for single organisms, and it is ideal for branching corals, or organisms with complex

98   morphological formations. The Flexi-chamber was robustly tested in the laboratory and field and

99   performed in line with other incubation chamber designs (Camp et al. 2015). However, the

100   chamber can only be used on substrates suitable for a cable tie attachment. For flatter substrates,

101   a domed benthic chamber design is more effective. The medium size chamber by Roth et al.

102   (2019) can be placed over the substrate and was successfully produced at a lower cost (~ $250

103   USD) than previous designs, while maintaining the efficiency and precision of more expensive

104   equipment. However, the design requires a bespoke rigid acrylic cylinder and a circulation pump

105   to recreate water movement inside the chamber, incurring a higher cost.

106   To contribute to the array of chambers currently available for field incubations, we designed a

107   chamber prototype, which was both low cost and suitable for deployment on complex substrates

108   incorporating small benthic communities to accurately measure community metabolism. Our

109   objectives were to design a benthic chamber that is; (1) low cost and easily constructed without

110   specialised equipment, (2) reproducible for scientific soundness, (3) minimally invasive to

111 reduce any impact on incubated organisms, (4) adaptable for use in a range of substrate types and

112   underwater environments, and (5) comparable with other chamber designs such as those

113   described in Table 1.

114

115   **Materials and Methods**

116   Study location

117   Experiments were carried out in the School of Geographical and Earth Sciences Laboratory at

118   the University of Glasgow, the Scottish Centre for Ecology and the Natural Environment

119   (SCENE) fieldwork site, and in Akumal Bay Natural Refuge Area, Mexico. SCENE is located

120   on the eastern shore of Loch Lomond in west central Scotland (56°07'41.1" N, 4°36'48.4" W).

121   Akumal is a small coastal town on the Caribbean coast of the Yucatan peninsula, with relatively

122   limited access to specialised materials. The Natural Refuge of Akumal Bay (20°23'42.2" N,

123   87°18'49.8" W) is a protected area within the Mexican Caribbean Biosphere Reserve and

124   consists of a semi-enclosed lagoon with patches of seagrass and coral ecosystems (Fig 1a). Field

125   experiments in Akumal were approved by the Comisión Nacional de Áreas Naturales Protegidas

126   (CONANP F009.DRBCM/240/2019).

127   Chamber design, materials, construction, and costs

128   The benthic chamber design consists of three key components: (1) a water-tight polyethylene

129   tent, (2) a sampling valve, and (3) a heavy yet malleable circular base for maintaining the tent

130   enclosure seal against the substrate (Fig. 1, Table 2). The tent is made from a polyethylene

131   plastic bag. It is possible to keep the shape of the plastic bag intact, by simply cutting in a

132   straight line at the bottom of the bag for the desired height, allowing an extra 10 – 15 cm at the

133   bottom to allow the circular malleable base to sit on top. Alternatively, a polyethylene bag or

134   sheet can be cut and re-sealed using a heat sealer into any desired enclosure shape, e.g., dome or

135   pyramid. For case study 1 the bottom of the bag was folded to create a 'skirt' for the base to sit

136   on. In case study 2 a dome shaped benthic chamber was used (Fig 1b, e), which was made by

137   cutting the polyethylene bag into panels and re-sealing using a heat sealer. We used a food

138   packaging heat sealer to join the panels. The valve was inserted by creating a small incision in

139   the enclosure tent and inserting one valve on the inside and securing it with the Luer lock

140   connector of a second valve on the inside. A small bicycle tube repair patch was used to create a

141   solid base for the valve to be inserted through. For the base, bicycle inner tubes were filled with

142   sand and fishing weights to create a heavy, malleable base, and re-sealed using bicycle tyre

143   repair kits found at a local hardware store. All materials to build the chamber were sourced

144   locally. Transparent polyethylene for the tent enclosure was bought from a local food packaging

145   company, Luer-lock valves were sourced in the local pharmacy and pre-used bicycle tyre inner

146   tubes were donated by the local community. The materials used and their associated costs are

147   summarised in Table 2.

148   Design validation

149   Three key characteristics were investigated to validate the reproducibility and correct functioning

150   of the chambers: (1) leakage of water from / to the chamber, (2) light transmission across the

151   plastic membrane, and (3) temperature stability within the chamber.

152   1.   Leakage

153   To test for leaks, non-toxic red food dye was inserted using a syringe (20ml) into a chamber

154   deployed over sediments in shallow water at each of our field sites. Visual surveys were

155   conducted by two snorkellers who monitored the water outside of the chamber for any obvious

156   visible leaks of red-dyed water for 30 minutes (Fig. 1c). An underwater camera (Canon

157   Powershot S120) was attached to a dive weight and placed on the substrate outside the chamber

158   for the duration of the 30-minute deployments, and the video was reviewed for any red dye

159   leakage around the base of the chamber. This process was repeated 3 times before case studies

160   and before lab testing. Following this initial coarse assessment, a 90-litre aquarium tank was

161   filled with artificial salt water (tap water prepared with Marine salts at a salinity of 21.5 ± 4.7

162   ppt.) and field water movement was simulated using 4 circulation pumps (Reef Tide 4000s 12v

163   DC Wavemaker Pump, UK) positioned on the sides of the tank to create a zig-zag water motion

164   across the tank. A prototype of the benthic chamber was placed in the tank and a super-saturated

165   saline solution was inserted using a plastic syringe connected to the valve of the benthic chamber

166   so that the water inside the chamber reached a salinity of 38.3 ± 5.7 ppt. Salinity was measured

167   once per minute during the 4-hour incubation, inside and outside the benthic chamber using two

168   cross-calibrated salinity loggers (Onset Hobo U24-002-C Saltwater Conductivity / Salinity Data

169   Logger). The leakage test was repeated 3 times, and for each repeat a different chamber was

170   used.

171   2. Light attenuation

172   A chamber was deployed over sediments in Akumal Bay at a depth of 2 m for 3 days between

173   07:00 and 19:00 hours in August 2019. A different chamber was used for each day of the

174   experiment (n=3). Photosynthetically active radiation (PAR) was measured simultaneously

175   inside and outside the chamber with two submersible sensors (Odyssey Submersible PAR

176   Logger) attached to a 4 kg dive weight and positioned inside and outside of each chamber to log

177   light each minute (μmol photons m^{-2} s^{-1}). The sensors were calibrated against a recently

178   calibrated Licor quantum sensor (LI-190, LI-COR Biosciences, US). Additionally, light

179   transmission (%) between the photosynthetically relevant wavelengths of 300 nm – 800 nm was

180   measured through the plastic membrane (Shimadzu UV-3600 UV-Vis).

181   3. Temperature

182   Changes to the temperature of water inside the chamber were measured to demonstrate

183   accumulation of heat, which we would expect to see if the water is not mixing well. Temperature

184   inside the chambers was collected using a handheld probe (Pro DSS multiparameter, YSI, US) at

185   the start and end of field deployments of 9 chambers in tropical conditions over 4 days in case

186   study 2. A separate 4-hour deployment in cold water conditions, at the SCENE fieldwork site in

187   Loch Lomond was also conducted in August 2021 and temperature was continuously logged for

188   the duration of the incubation (per minute) inside and outside of the chamber using temperature

189   loggers (Onset HOBO UA-002-08 Pendant 8K Light and Temperature) with an accuracy of $\pm$

190   0.5°C.

191   Field operation of the benthic chamber

192   Field deployments over benthic communities were conducted to validate the reproducibility and

193   adaptability of the chambers. Two case studies were conducted in Akumal Bay (Fig. 1d), one

194   with incubations of seagrass patches and the other over coral reef communities (total of 41

195   deployments). Chambers were installed by divers and snorkellers. For all field incubations, water

196   samples were extracted at the start and end of 1.5 to 3.5-hour long incubations using 100 ml

197   plastic syringes with a Luer-lock connection to the chamber valve. Dissolved oxygen, pH,

198   temperature, and salinity were measured using a handheld non-submergible multiparameter

199   sensor (ProDSS equipped with ODO Optical Dissolved Oxygen and EXO pH Smart Sensors,

200   YSI, US) attached to a kayak for analysis of samples within 1 minute of extraction. Chambers

201   were flushed between incubations times by lifting them from the substrate and releasing the

202   incubated water. A few minutes were allowed for any stirred-up sediments to re-settle before

203   reassembling the chamber. Repeated measurements (n=15) of chamber volume were conducted

204   in shallow (<1 meters) of Akumal Bay by filling chambers using a 100 ml syringe and recording

205   variability between volumes to estimate error in volume measurements.

206   Adaptations of the chamber

207   A more streamlined, low-profile, dome-shaped chamber (Fig. 1b) was used due to higher surge

208   at the coral reef site, nearer to the reef crest than the protected seagrass area (Fig. 1d). This was

209   also an adaptation for the lower profile of reef patches (~15 cm height) compared to seagrasses

210   (~ 30 cm height). The panels were cut as curved triangles (29 x 16 cm, H x W) with arching

211   sides and each dome was constructed of 8 panels and two 8 cm skirts were added at the base.

212   These skirts were added due to higher wave action at this site, to prevent leakage around the seal.

213   All plastic seams were sealed with a double seal 1 cm apart on each joint, using a generic, locally

214   available heat sealer. For the high-energy environment (case study 2) a heavier base was created

215   by adding 8 kg of fishing weights into the bicycle tyre tube to total ~10 kg per base. Chambers

216   were randomised over the substrate types for each incubation; algae-, coral-, and sand-

217 dominated. Incubations lasted 3.5 hours. PAR was measured as described above in both case

218 studies.

219 Case study 1: Seagrass production

220 Benthic chambers (n=5) were assembled and deployed over seagrasses and sediment substrate at

221 1.5 to 2 m depth. Seagrass surveys were conducted using the methods outlined in Hernández and

222 Tussenbroek (2014) to estimate seagrass abundance in Akumal Bay (Fig. 1d). Sampling was

223 conducted at the start and end of incubations at midday, late afternoon, and after dark. Each

224 incubation lasted 1.5 to 2.5 hours. The chamber constructed for the seagrasses (Fig. 1c) was

225 taller and narrower than the chamber used in case study 2 (Fig. 1b) to accommodate the height of

226 the seagrasses.

227 Case study 2: Production rates of distinct coral reef communities

228 Benthic chambers (n=9) were deployed by SCUBA divers at 2-3 m depth over four days for

229 multiple incubations during solar noon and after dark over small patches of reef. Using swim

230 patterns from a central point ('Case study 2' label on Fig. 1d), small patches of mixed coral

231 (*Porites spp.*), algae, crustose coralline algae, and sand/sediment were identified (n=21), of

232 which 9 were randomly selected for incubation. Surface area and volume of the incubated reef

233 patches were measured using photogrammetry. 3D models of incubated reef patches were

234 constructed from ~100 photographs of each patch using Agisoft Metashape and compared

235 following the methods outlined in Lange and Perry (2020). Surface areas (m^2) and volume (m^3)

236 were extracted from the 3D models. We converted the volume to litres and deducted it from the

237 chamber volume to calculate the individual sea water volume for each incubation and used this,

238   with the surface area measurement to normalise metabolic rates. All areas of flat sediment were

239   measured from top-down photos using ImageJ (Schneider et al. 2012).

240   Metabolism calculations

241   Net community production (NCP, mmol m^{-2} hr^{-1}) was calculated from changes to dissolved

242   oxygen (DO) using the following equation:

243   (Eq. 1)

244   $$NCP = \frac{\Delta DO \times V}{SA \times T}$$

245   where ΔDO is the change in dissolved oxygen (mmol L^{-1}), which is normalised to the chamber

246   volume (V) of water in litres, the surface area (SA) of the incubated sample in m^2, and the

247   incubation duration time (T) in hours. Surface area was measured from 3D models using the

248   program Agisoft following the protocol outlined in Lange and Perry (2020). Individual chamber

249   seawater volumes (V) were calculated by converting the estimated organism volume extracted

250   from 3D models (m^3) into litres (L) and subtracting this from the empty chamber seawater

251   volume. Dissolved oxygen fluxes were normalised to individual chamber water volumes and

252   organism surface areas.

253   Photosynthesis-Irradiance models

254   Rates of productivity (NCP) were modelled to light using the hyperbolic tangent equation of

255   Jassby and Platt (1976):

256   (Eq. 2)

257
$$P_{net} = P_{max} \times \tanh\left(\frac{\alpha \times E}{P_{max}}\right) + R$$

258   where P_{net} is the modelled net production rate (mmol m^{-2} hr^{-1}), R is the average dark respiration

259   rate (mmol m^{-2} hr^{-1}), and E is irradiance in PAR (μmol photons m^{-2} s^{-1}). The coefficients derived

260   from the model include: the initial slope (α) between NCP and light and the maximum gross

261   photosynthetic rate (P_{max}).

262   Statistical analysis

263   Statistical analyses were carried out using RStudio version 1.4.1717 (R Core Team 2021) with

264   the package *Tidyverse* (Wickham, 2019). Each data set was assessed for parametric assumptions

265   using Shapiro Wilkes, Q-Q plots, and histograms. Data did not always meet the assumptions of

266   normality; therefore, nonparametric statistical tests were selected for the analyses. For testing of

267   chamber parameters (light, pH, temperature, leakage), paired sign tests and Wilcoxon rank sum

268   tests with continuity correction were used, and for the case studies Kruskal Wallace tests were

269   used to compare mean rates of NCP at different times of day and between different benthic

270   communities. Linear regressions of seagrass NCP with light were modelled using *ggplot* with

271   *ggpmisc* extension on R (Wickham 2016; Aphalo 2021). Photosynthesis - irradiance curves were

272   modelled using R nonlinear least squares estimation and coefficients / model fit were evaluated

273   based on R^2, confidence intervals, and standard error of the regression (sigma, σ).

274

275   **Results**

276   Construction of benthic chambers for field deployment

277   Benthic chambers (*n=6*) were successfully constructed and deployed by citizen scientists in the

278   seagrass meadow of Akumal Bay in July 2019. Materials were sourced locally and the cost per

279   chamber was USD $17.62. Details on costs for the items are included in Table 2. The time taken

280   to fill rubber tubes with sand and weights, cut the plastic bag, and install a valve ranged from 15

281   to 30 minutes for 2 people and 45 minutes for 1 person. The chambers were deployed without

282   difficulty by a range of users of varying experience.

283   Leakage

284   Salinity inside the chamber at the start of the incubations (38.9 ± 0.3 ppt; mean ± SD) was

285   reduced by 0.8 ± 0.3 ppt over the course of the 4-hour incubations. Overall, the difference in

286   salinity was -2.1 ± 0.8 % between the start and end values of 3 replicate incubations during 4-

287   hour incubations. The salinity of the water outside the chamber remained stable throughout the

288   incubations (26.1 ± 0.1 ppt.).

289   Transparency

290   Laboratory testing found that light transmission through the polyethylene plastic was 74.4 % at

291   750 nm and 61.1 % at 400 nm (Fig. 2a). In the field, the difference between PAR measured

292   simultaneously inside and outside the chamber over 3 field deployments was 13.0 % ± 1.9 (mean

293   ± SD) and the difference was only found to be significant over 2 hours at peak sun on 2 days

294   (Wilcoxon signed rank test with continuity correction, Table S1).

295   Temperature

296   Seawater temperatures measured inside (30.7 ± 0.7 °C, median ± SD) and outside chambers

297   (30.7 ± 0.8 °C, *n* = 9) at the end of 3-hour incubations in peak sun were not significantly

298   different (Sign test statistic = 18, df = 28, p =0.185).

299   Case Study 1: Seagrass productivity rates increase with peak sunlight

300   Six benthic chambers were deployed over a seagrass-sediment substrate in Akumal Bay.

301   Seagrass coverage was composed of three species: *Thalassia testudinum, Syringodium filiforme,*

302   and *Halodule wrightii*, and visual surveys indicated 50% areal coverage within the incubation

303   area. Increases in DO concentration demonstrated positive net community productivity (NCP)

304   during daylight incubations, while negative NCP after sunset indicated net respiration for all

305   seagrass incubations (Fig. 3). All values presented as mean ±SD. The difference in dissolved

306   oxygen (ΔDO) was 78.5 ± 7.5 µmol L^{-1} at solar noon when concentrations of 272.5 ±7.5 µmol L^{-1}

307   ^{1} DO were reached and during night incubations fell to 186.8 ±12.7 µmol L^{-1} DO with an

308   average ΔDO of -45.2 ±12.7 µmol L^{-1}. NCP was significantly different during different times of

309   the day (KW = 13.3, df = 2, p = 0.00126). Average NCP was highest at solar noon (6.7 ±1.3

310   mmol m^{-2} hr^{-1}), lower in the late afternoon (2.4 ± 0.6 mmol m^{-2} hr^{-1}) and negative after sunset (-

311   3.3 ± 0.4 mmol m^{-2} hr^{-1}). Seagrass NCP had a strong linear relationship with PAR (R^2 = 0.93, p =

312   <0.0001). One incubation done over sediments (n=1) also had the highest NCP rate at solar noon

313   (2.6 mmol m^{-2} hr^{-1}) and was negative at night (-0.6 mmol m^{-2} hr^{-1}).

314   Case Study 2: Measuring productivity of coral-algae reef patches

315   Compositions of 9 small patches of reef (planar surface area = 1075.2 cm^2) were described by

316   relative proportions of functional groups such as coral, macroalgae, crustose coralline algae, and

317   sediment measured from 3D models (Figs. 4 & 5). Two patches consisted of sediments only, 3

318   were algae-dominated, and 4 were coral-dominated. One of the coral-dominated patches

319   consisted of a coral, which had begun to bleach. Surface areas calculated from 3D models were

320   2.86 ± 1.04 m^2. Chamber seawater volumes averaged (mean ±SD) 15.72 ± 2.86 L (Table 3).

321   NCP was generally positive during daytime incubations and negative at night for all substate

322   types (Kruskal-Wallace statistic = 49.9, df = 1, p = 1.61 x 10^{-12}). NCP rates measured from the 9

323   distinct patches were different during the daytime (Kruskal-Wallace statistic = 25.0, df =8, p =

324   0.002) and at night (Kruskal-Wallace statistic = 19.2, df =8, p = 0.014). When the patches were

325   categorised into algae-, coral-, and sand-dominated groups, pairwise comparisons revealed that

326   NCP was different between sand - algae and coral – algae, but algae and coral did not have

327   significantly different NCP during the day or at night (Table 4).

328   Photosynthesis-irradiance data fit a hyperbolic relationship with PAR for all substrates (Fig. 6).

329   Photosynthetic maximum (P_{max}) was highest in the algae-dominated substrate type (11.6 ± 0.9

330   mmol m^{-2} hr^{-1}) and lowest for sand/sediments (4.2 ± 0.6 mmol m^{-2} hr^{-1}). All model coefficients

331   were significant (Table 5).

332   **Discussion**

333   We designed and tested a novel benthic incubation chamber, drawing together key principles

334   from existing designs (e.g., Yates & Halley 2003; Camp et al., 2015; Roth et al. 2019). The

335   benthic chamber was designed to incubate small communities, single organisms, or sediments.

336   The equipment created was low cost, reproducible, minimally invasive, and adaptable, with

337   comparable features and capabilities to other in-situ benthic incubation chambers (*see* Table 1).

338   The chambers were successfully assembled and deployed for fieldwork by citizen scientists and

339   students. Construction of a single benthic chamber took between 15 to 30 minutes for two

340   people, including the time taken to measure the volume of the chamber and to fill the tube base

341   with sand. In the water, deployment over complex substrate took 5 minutes or less by two

342   qualified divers. The performance of the chambers was evaluated by conducting productivity

343   measurements using field deployments of the chambers over as a seagrass bed (case study 1), as

344   well as algae, coral, and sand dominated reef patches (case study 2). The results obtained using

345   this method were comparable to those obtained in previous studies using established chambers

346   designs, demonstrating the effectiveness and feasibility of the chamber design as a low-cost

347   alternative for benthic incubations. Lowering the costs of in-situ incubation apparatus broadens

348   the accessibility and scope for measurements of benthic metabolism for conservation monitoring

349   purposes.

350   Evaluating the chamber design

351   The benthic chamber design presented in this study is novel in its accessibility and scope for

352   implementation with limited resources. Benthic incubations allow for direct measurements of

353   benthic metabolism and are an important tool for quantifying carbon fluxes from physiological

354   processes within benthic communities. However, the most inexpensive chambers currently

355   available for in-situ community incubations cost around USD $200 to build and require bespoke

356   parts and a submersible pump for operation (Roth et al. 2019), while the economical 'flexi-

357   chamber' (Camp et al. 2015) is limited to individual coral colonies, rather than benthic

358   communities. The chamber presented in the current study incubates communities or individuals

359   and it costs < USD $20 to construct. At such low costs, multiple replicates are feasible. The

360   training required to build, deploy, and collect data using most chamber designs is not yet widely

361   available. We demonstrated that the flux measurements can be normalised to surface area and

362   volume data either using more traditional estimates of planar area and percentage cover in case

363   study 1 or using a 3D modelling approach as in case study 2. This demonstrates the adaptability

364   of our chamber design for example when the software and computational power required for the

365   latter technique may not be available. The benthic chamber itself does not require any specialised

366   equipment or training to deploy as materials were locally sourced and citizen scientists were able

367   to make and deploy the chambers with minimal training.

368 We demonstrated that the novel chambers can be constructed from locally sourced materials

369 without the need for any specialised parts. Plastic bags, bicycle inner tubes, fishing weights, and

370 SCUBA gear for underwater transport were all easily sourced on site. We purchased Luer-lock

371 valves from a local medical supply store, however, we also trialled the chamber construction and

372 deployment with a plastic sports bottle cap instead of the valve (Fig. 1c). The chamber in this

373 study was constructed for less than USD $20, however it should be noted that the sensors used to

374 measure dissolved oxygen, pH, and salinity inside the chambers should be considered as an

375 additional cost. This is true of all but one of the selected chambers in Table 1 and would be

376 dependent on the individual experiment being conducted with the benthic chamber and the

377 precision and accuracy required.

378 To verify the reproducibility of the chamber design for determining photosynthesis, we

379 conducted net community productivity measurements. First, we measured light attenuation of the

380 polyethylene tent and found a reduction of 13% ± 1.9 between inside and outside the chamber

381 (Fig. 2b). These results aligned with the transparency of comparable chambers, such as the 9%

382 reduction in light reported in Roth et al. (2019) and 16% in Camp et al. (2015). Our results

383 support previous findings that transparent plastic polyethylene or vinyl materials sourced at food

384 packaging, hardware, or medical supply stores are effective for incubations of photosynthetic

385 organisms (Yates and Halley 2003; Camp et al. 2015). As the chamber is adaptable for distinct

386 locations, uses, and resources, light attenuation should be measured given the variability in light

387 transmission by different plastics.

388 One of the unique features of the novel chamber design is the malleable base, which facilitates

389 deployment over hard, uneven substrate without using destructive methods to fix the chamber in

390 place. This is particularly useful for incubations in managed or protected areas, where attachment

391 by digging the chamber base into sediments or pinning the chamber to a coral reef using nails or

392 cable tie attachments might not be feasible. The rubber tubing base was weighted with easily

393 available materials to create a seal with the substrate, which could be adapted to 3D structure on

394 the reef incurring minimal damage. Given that the malleable base could be a potential source of

395 leakage, laboratory testing was conducted, and we demonstrated that the rate of water exchange

396 was 2% over 4 hours. We consider the novel benthic chamber to be a reproducible method and

397 effective for accurate measurement, based on the results of laboratory testing and case studies.

398 Water exchange during field deployments may vary, depending on the local conditions, for

399 example surge, currents, and substrate type, therefore it is advisable that users of the chamber

400 incorporate a testing phase to adjust the weight of the base to ensure that it is sufficient to create

401 a seal. Users could replicate the salinity method by adding hypersaline solution to the chamber

402 and measuring salinity at the start and end of the incubation time (Webb et al. 2021), or an

403 alternative if refractometers are not available would be the visual assessment of leakage using

404 non-toxic food dye. It is also possible to visually assess water mixing and movement using dye.

405 We injected red food dye into field-deployed chambers and observed full dispersal within one

406 minute (Fig. 1c).

407 Water movement over the reef is a driver of metabolic fluxes (Comeau et al. 2014; 2019) and

408 maintaining natural water movement without the restriction of a solid chamber wall sustains

409 ambient in-situ conditions throughout the sampling period. The flexibility of the plastic bag

410 material used for the tent enclosure also has the benefit of reducing costs compared to rigid

411 chambers by encouraging natural water movement and mitigating the need for a submersible

412 pump inside the chamber. The concept of using a flexible plastic enclosure was demonstrated

413 with the Flexi-chamber design (Camp et al. 2015). While the flexibility of the tent enclosure

414   promotes natural water movement and mixing, any benthic chamber will disrupt natural water

415   movement, which should be considered when interpreting data collected with benthic chambers

416   in general. The NCP rates measured in our case studies also demonstrate that water movement is

417   maintained by the flexible walls, as supported by the NCP rates measured (discussed below).

418   The benthic chamber used in this study is adaptable to different substrate types, environmental

419   conditions, and research applications. The simple and flexible design enables easy adjustment of

420   size and volume, and additional valves or sampling ports can be easily installed. The chamber

421   can be used to measure additional parameters to those measured in this study, for example, to

422   collect sea water samples for carbonate chemistry to measure calcification rates. This may add to

423   the expertise and costs of using the chamber. The weight of the base can be altered for high or

424   low energy systems, and the height of the dome can also be changed to accommodate different

425   samples sizes and heights. It can also be adjusted to enhance or minimise hydrodynamic mixing

426   by naturally occurring currents or wave action. As the base is malleable, it can be used on hard

427   substrate or soft sediments as demonstrated in our case studies over reef communities and

428   seagrass beds. The two case studies demonstrated the adaptability of the chamber.

429   Seagrass productivity measured with the benthic chambers

430   Incubations over seagrass and sand demonstrated a typical diel trend of NCP increasing with

431   sunlight and switching to net respiration at night. Seagrass productivity rates were in line with

432   those of previous studies measuring seagrass NCP, however, variability does exist (Duarte et al.

433   2010). The average solar noon NCP rate measured in this study (6.7 ± 1.3 mmol m^{-2} hr^{-1}) was

434   lower than NCP measured in Florida with the SHARQ chamber (12.3 ± 1.0 mmol m^{-2} hr^{-1}, Turk

435   et al., 2015). However, our rates were higher than the average NCP for tropical Western Atlantic

436   seagrass meadows described in a meta-analysis by Duarte et al. (2010) in which daily NCP

437 averaged 23.7 ± 7.8 mmol m^{-2} day^{-1} over 155 seagrass studies, which would equate to an hourly

438 rate of approximately 2.2 mmol m^{-2} hr^{-1}. Seagrasses in Akumal Bay are colonised by epiphytes

439 and cyanobacteria (Hernández and Tussenbroek 2014), associated with high nutrient load in the

440 bay, which may have influenced our NCP measurements (Coleman and Burkholder 1994;

441 Borowitzka et al. 2007). Productivity increased linearly with light and did not reach

442 photosynthetic saturation. Therefore, it was not possible to fit the hyperbolic tangent equation,

443 possibly due to the limited light conditions in the study design (i.e., there were only 2 light

444 levels).

445 Measuring productivity of coral -algae reef patches

446 Net production rates measured for all reef patches were positive during light incubations and

447 negative for dark incubations in line with previous studies of in-situ coral reef metabolism

448 measured with benthic chambers. For example, light NCP measured with the SHARQ enclosure

449 at a reef site in Florida averaged 8.6 ± 1.0 mmol m^{-2} hr^{-1} (Turk et al. 2015), a rate that also

450 aligned with NCP measured estimated by CROSS (McGillis et al. 2011), and previous SHARQ

451 deployments within the Caribbean region (Turk et al. 2015). Our night respiration rates,

452 measured from around dusk until $21:00 - 22:00$ hours, were also in agreement with the values

453 measured in the early evening using SHARQ deployments in Turk et al. (2015). The highest

454 rates of NCP were measured in coral patch 3, which was the only replicate containing *P.*

455 *astreoides* as well as *P. porites*. Net community production was lowest in patch containing a

456 bleached *P. porites* colony ('Coral 4'on Fig. 5), which had been subjected to heavy

457 sedimentation and algal overgrowth. The lower rates of NCP measured in the incubations of this

458 colony most likely reflect lower metabolic rates due to environmental stress. Coral patches 1 and

459 2 were very similar in terms of the health, size, and structure of the *P. porites* colonies incubated

460   and they had minimal (<10%) algae within the chambers, as reflected by the similar rates

461   measured in these incubations. We modelled reef NCP data to light and found a hyperbolic

462   relationship between PAR and NCP as have other studies (Long et al., 2013; Takeshita et al.,

463   2016; Turk et al., 2015). However, our modelling approach was somewhat limited by the range

464   of light levels and number of incubations. Future research should aim to include more

465   incubations at different times of day. The low costs of the chamber we present in this study

466   supports such research.

467   **Conclusions**

468   Monitoring of coastal ecosystem health is of critical importance for tracking and predicting

469   ecological response to global climate change and other localised threats. This study presents a

470   novel benthic chamber design, which reduces the cost of in-situ incubations of benthic organisms

471   in shallow coastal ecosystems, while maintaining reproducibility. The chamber was designed to

472   be minimally invasive and adaptable, which we demonstrate through successful field

473   deployment. We measured productivity rates for seagrasses and reef patches in line with

474   previous studies and provide a comparison of rates. Further studies are needed for quantification

475   of coastal carbon cycling and efficient methods to enhance conservation monitoring, and the

476   low-cost benthic chamber we describe overcomes some of the limitations of other designs. It is a

477   potential tool for diverse users to employ in such research endeavours.

478

479   **Acknowledgements**

480   Data collection, logistics and planning were conducted with the support of Operation Wallacea

481   scientists Sabrina Weber, Jessica Rose-Innes, Holly Jones, Dr Gemma Fenwick, Dr Kathy Slater,

482   and other staff and student research assistants who were generous with their time building and

483   trialling the chambers. We thank the Akumal Dive Center's skilled team of divers, captains, and

484   staff for their valuable practical advice and logistical support. Thank you to team Coralium,

485   UNAM for help with sourcing local materials, to Charlotte Slaymark, Kenny Roberts, and

486   Jessica Walker at the University of Glasgow for technical support in the laboratory and to the

487   team at SCENE for facilitating field testing in Scotland. A special thank-you to the Hotel

488   Akumal Caribe for hosting and to the Coral Conservation Society for facilitating this research.

489

490   **References**

491   Albright, R., J. Benthuysen, N. Cantin, K. Caldeira, and K. Anthony. 2015. Coral reef

492   metabolism and carbon chemistry dynamics of a coral reef flat. Geophys. Res. Lett. **42**:

493   3980–3988. doi:10.1002/2015GL063488

494   Aphalo, P. J. 2021. ggpmisc: Miscellaneous Extensions to "ggplot2".

495   Barnes, D. J. 1983. Profiling coral reef productivity and calcification using pH and oxygen

496   electrodes. J. Exp. Mar. Biol. Ecol. **66**: 149–161. doi:10.1016/0022-0981(83)90036-9

497   Berg, P., M. L. Delgard, P. Polsenaere, K. J. McGlathery, S. C. Doney, and A. C. Berger. 2019.

498   Dynamics of benthic metabolism, O_2, and pCO_2 in a temperate seagrass meadow. Limnol.

499   Oceanogr. **64**: 2586–2604. doi:10.1002/LNO.11236

500   Berg, P., Huettel, M., Glud, R.N., Reimers, C.E. and Attard, K.M., 2022. Aquatic eddy

501   covariance: the method and its contributions to defining oxygen and carbon fluxes in marine

502   environments. Annual review of marine science, 14. https://doi.org/10.1146/annurev-

503   marine-042121012329

504   Borowitzka, M.A., Lavery, P.S. and Van Keulen, M., 2006. Epiphytes of seagrasses. *In*

505   Seagrasses: biology, ecology and conservation. (Eds. AW D. Larkum, RJ Orth, and CM

506   Duarte.) pp. 441--61.

507   Camp, E. F., S.-L. Krause, L. M. F. Santos, M. S. Naumann, R. K. P. Kikuchi, D. J. Smith, C.

508   Wild, and D. J. Suggett. 2015. The "Flexi-Chamber": A Novel Cost-Effective In Situ

509   Respirometry Chamber for Coral Physiological Measurements. PLoS One **10**: e0138800.

510   doi:10.1371/journal.pone.0138800

511   Coleman, V. L., and J. A. M. Burkholder. 1994. Community structure and productivity of

512   epiphytic microalgae on eelgrass (*Zostera marina* L.) under water-column nitrate

513   enrichment. J. Exp. Mar. Biol. Ecol. **179**: 29–48. doi:10.1016/0022-0981(94)90015-9

514   Comeau, S., C. E. Cornwall, C. A. Pupier, T. M. DeCarlo, C. Alessi, R. Trehern, and M. T.

515   McCulloch. 2019. Flow-driven micro-scale pH variability affects the physiology of corals

516   and coralline algae under ocean acidification. Sci. Rep. **9**: 1–12. doi:10.1038/s41598-019-

517   49044-w

518   Comeau, S., P. J. Edmunds, C. A. Lantz, and R. C. Carpenter. 2014. Water flow modulates the

519   response of coral reef communities to ocean acidification. Sci. Rep. 41 **4**: 1–6.

520   doi:10.1038/srep06681

521   Cyronak, T., A. J. Andersson, C. Langdon, et al. 2018. Taking the metabolic pulse of the world's

522   coral reefs. PLoS One **13**: e0190872. doi:10.1371/journal.pone.0190872

523   Duarte, C. M., N. Marbà, E. Gacia, J. W. Fourqurean, J. Beggins, C. Barrón, and E. T.

524   Apostolaki. 2010. Seagrass community metabolism: Assessing the carbon sink capacity of

525   seagrass meadows. Glob. Biogeochem. Cycles **24**: 1–8. doi:10.1029/2010GB003793

526 Duarte, C. M., T. Sintes, and N. Marbà. 2013. Assessing the CO_2 capture potential of seagrass

527   restoration projects. J. Appl. Ecol. **50**: 1341–1349. doi:10.1111/1365-2664.12155

528 Falter, J. L., R. J. Lowe, M. J. Atkinson, S. G. Monismith, and D. W. Schar. 2008. Continuous

529   measurements of net production over a shallow reef community using a modified Eulerian

530   approach. J. Geophys. Res. **113**: 7035. doi:10.1029/2007JC004663

531 Hernández, A. L. M., and B. I. van Tussenbroek. 2014. Patch dynamics and species shifts in

532   seagrass communities under moderate and high grazing pressure by green sea turtles. Mar.

533   Ecol. Prog. Ser. **517**: 143–157. doi:10.3354/MEPS11068

534 Huettel, M. and Gust, G., 1992. Solute release mechanisms from confined sediment cores in

535   stirred benthic chambers and flume flows. Marine ecology progress series. Oldendorf,

536   82(2), pp.187-197. doi: 10.3354/meps082187

537 Jassby, A. D., and T. Platt. 1976. Mathematical formulation of the relationship between

538   photosynthesis and light for phytoplankton. Limnol. Oceanogr. **21**: 540–547.

539   doi:10.4319/lo.1976.21.4.0540

540 Kline, D. I., L. Teneva, K. Schneider et al. 2012. A short-term in situ CO_2 enrichment

541   experiment on Heron Island (GBR). Sci. Rep. **2**: 413. doi:10.1038/srep00413

542 Lange, I. D., and C. T. Perry. 2020. A quick, easy and non-invasive method to quantify coral

543   growth rates using photogrammetry and 3D model comparisons Methods Ecol. Evol. **11**:

544   714–726. doi: 10.1111/2041-210X.13388

545 Lange, I. D., C. T. Perry, and L. Alvarez-Filip. 2020. Carbonate budgets as indicators of

546   functional reef "health": A critical review of data underpinning census-based methods and

547 current knowledge gaps. Ecol. Indic. **110**. doi:10.1016/j.ecolind.2019.105857

548 Long, M. H., P. Berg, and J. L. Falter. 2015. Seagrass metabolism across a productivity gradient

549  using the eddy covariance, Eulerian control volume, and biomass addition techniques. J.

550  Geophys. Res. Oceans **120**: 3624–3639. doi:10.1002/2014JC010352

551 McGillis, W. R., C. Langdon, B. Loose, K. K. Yates, and J. Corredor. 2011. Productivity of a

552  coral reef using boundary layer and enclosure methods. Geophys. Res. Lett. **38**: n/a-n/a.

553  doi:10.1029/2010GL046179

554 Murphy, B. A., C. H. Mazel, R. Whitehead, and A. M. Szmant. 2012. CISME: A self-contained

555  diver portable metabolism and energetics system. *OCEANS 2012 MTS/IEEE: Harnessing*

556  *the Power of the Ocean*. doi**:** 10.1109/OCEANS.2012.6405075

557 Olivé, I., J. Silva, M. M. Costa, and R. Santos. 2016. Estimating Seagrass Community

558  Metabolism Using Benthic Chambers: The Effect of Incubation Time. Estuaries Coast. **39**:

559  138–144. doi:10.1007/s12237-015-9973-z

560 R Core Team. 2021. R: A language and environment for statistical computing. R Foundation for

561  Statistical Computing Title.

562 Roth, F., C. Wild, S. Carvalho, and others. 2019. An in situ approach for measuring

563  biogeochemical fluxes in structurally complex benthic communities C. Trueman [ed.].

564  Methods Ecol. Evol. **10**: 712–725. doi:10.1111/2041-210X.13151

565 Schneider, C. A., W. S. Rasband, and K. W. Eliceiri. 2012. NIH Image to ImageJ: 25 years of

566  image analysis. Nat. Methods **9**: 671–675. doi:10.1038/nmeth.2089

567 Shaw, E. C., S. R. Phinn, B. Tilbrook, and A. Steven. 2014. Comparability of slack water and

568 Lagrangian flow respirometry methods for community metabolic measurements. PLoS One

569 **9**: e112161. doi:10.1371/journal.pone.0112161

570 Takeshita, Y., W. McGillis, E. M. Briggs, A. L. Carter, E. M. Donham, T. R. Martz, N. N. Price,

571 and J. E. Smith. 2016. Assessment of net community production and calcification of a coral

572 reef using a boundary layer approach. J. Geophys. Res. Oceans **121**: 5655–5671.

573 doi:10.1002/2016JC011886

574 Turk, D., K. Yates, M. Vega-Rodriguez, and others. 2015. Community metabolism in shallow

575 coral reef and seagrass ecosystems, lower Florida Keys. Mar. Ecol. Prog. Ser. **538**: 35–52.

576 doi:10.3354/meps11385

577 van Heuven, S. M. A. C., A. E. Webb, D. M. de Bakker, E. Meesters, F. C. van Duyl, G.-J.

578 Reichart, and L. J. de Nooijer. 2018. In-situ incubation of a coral patch for community-scale

579 assessment of metabolic and chemical processes on a reef slope. PeerJ **6**: e5966.

580 doi:10.7717/peerj.5966

581 Webb, A. E., D. M. de Bakker, K. Soetaert, T. da Costa, S. M. A. C. van Heuven, F. C. van

582 Duyl, G.-J. Reichart, and L. J. de Nooijer. 2021. Quantifying functional consequences of

583 habitat degradation on a Caribbean coral reef. Biogeosciences **18**: 6501–6516.

584 doi:10.5194/BG-18-6501-2021

585 Wickham, H. 2016. ggplot2: Elegant Graphics for Data Analysis.

586 Wickham, H. 2019. Welcome to the tidyverse. J. Open Source Software, 4(43): 1686

587 Wild, C., Rasheed, M., Jantzen, C., Cook, P., Struck, U., Huettel, M. and Boetius, A., 2005.

588 Benthic metabolism and degradation of natural particulate organic matter in carbonate and

589   silicate reef sands of the northern Red Sea. Marine Ecology Progress Series, 298, pp.69-78.

590   doi:10.3354/meps298069

591   Yates, K. K., and R. B. Halley. 2003. Measuring coral reef community metabolism using new

592   benthic chamber technology. Coral Reefs **22**: 247–255. doi:10.1007/S00338-003-0314-5

593

594   .

Summary of the key features of selected benthic chamber designs since 2000.

Benthic chamber designs were selected to incorporate a size gradient ranging from sub-organism to community incubations. We selected studies which evaluate the performance of the chambers. This table is not exhaustive and only provides a summary of chamber types.

	Name	Scale	Cost (USD)	Leakage	Light trans.	Strengths	Limitations
	Coral In-Situ Metabolism and Energetics (CISME), (Murphy et al. 2012)	< 1 individual	$32,000	Unreported, expected minimal	0% (Artificial light)	High accuracy and precision. Instantaneous measurements	Expensive and specialised. Very small areas can be incubated (24.5 cm^2).
	Flexi-Chamber (Camp et al. 2015)	Single	< $20	None-to-minimal	84%	Low-cost and easily sourced materials. Flexible material maintains water movement.	Cable tie closure around the base is not suitable for all benthic organisms.
	Flexi-community benthic chamber for remote locations, *this study*	Single small community	<$20	2% over 4 hours	89%	Low-cost, easily sourced materials. Adaptable design. Flexible material maintains water movement.	Under some conditions seal is not as reliable as other methods.
	In-situ chambers for measuring biogeochemical fluxes (Roth et al. 2019)	Single small community	~$250	5.3% within 6 hr (reef sands) 12.4% within 6 hr (rocky)	92%	Can be deployed on hard substrate or sediments.	Requires circulation pump. Bespoke design requires specific materials.
	Submersible Habitat for Analyzing Reef Quality (SHARQ) (Yates & Halley 2003)	Larger communities (~12 m^2 planar surface area)	Not reported	Variable depending on substrate type	>71%	Can incubate entire communities.	Requires circulation pump. Bespoke design requires specific materials.

Summary of key chamber design components.

	Key features	Materials and costs (USD)	Adaptations
Tent enclosure	Plastic retains upright structure due to neutrally buoyancy, while its flexibility allows movement with water, facilitating mixing and flow. If needed, watertight glue or silicone can be used along the vertical seams to provide a more rigid upright structure.	Transparent polyethylene bags were sourced from local food packaging and grocery stores for $0.25 per unit in Mexico, and for approx. $1.80 per unit in the UK. Glue and silicone for re-sealing were sourced at local hardware stores for <$5, with an estimated cost of $0.50 per chamber.	Size of plastic bag can be changed to incubate different volumes of water or surface areas of substrate Enclosure transparency or colour filtration can be achieved with different plastics. The shape of chamber can be adapted for high-energy settings.
Sampling valve	A valve was installed into each chamber for the extraction of water samples with syringes. Installation involved a pinprick hole in the plastic, with a valve Luer-lock inserted and attached to a second Luer-lock valve on the inside of the chamber.	The valves tested in this study were 3-way Luer-lock valves, priced at $1.12 per unit. In lieu of valves, sports bottle caps can be implemented at a similar cost.	A sampling port of any size can be installed, depending on study requirements. 3-way valves can facilitate the addition of experimental treatments. The location of the valve on the chamber could impact mixing.
Base	The heavy chamber base is placed on top of the plastic enclosure skirt to create a seal with the substrate. The base is malleable so that it can be moulded to the complexity of solid substrates, and in the case of soft substrata, buried as needed.	Bicycle inner tubes were cut to size and filled with sand and small fishing weights. After filling, the tubes were sealed using bicycle tyre patches and glue. As the used bicycle tubes were donated there was no cost. New inner tubes cost ~$4 each. Fishing weights $3 per kg.	Base weight can be adjusted as needed, depending on the environmental conditions. Stones can be used in lieu of fishing weights.

Measurements of benthic chamber and incubated coral reef patches.

Surface areas in square metres (m^2) and sea water volume in litres (L) of incubated reef patches estimated from 3D models following the protocol outlined by Lange and Perry (2020). Substrate type refers to the pre-dominant functional group.

Patch	Substrate type	Replicate	Surface area (m^2)	Seawater volume (L)
1	Sand	1	1.14	20.00
2	Sand	2	1.22	20.00
3	Algae	1	2.24	13.26
4	Algae	2	2.43	15.55
5	Algae	3	3.20	12.82
6	Coral	1	1.77	15.41
7	Coral	2	2.73	16.20
8	Coral	3	1.03	17.27
9	Bleached coral	4	4.39	11.769

Comparison of net community production (NCP) rates between coral reef patches using non-parametric Wilcox pairwise comparisons.

Rates of NCP (in mmol m^{-2} hr^{-1}) were compared between the different types of reef patches incubated in case study 2 (coral-, algae- and sand- dominated substrates) at day and at night. Significance level represented by stars (*) refers to the p-adjusted values, and 'ns' is an abbreviation for not significant.

	Group 1	Group 2	n_1	n_2	Statistic	P value	Adjusted p value	Significance
Day	Algae	Coral	12	14	67	0.4030	0.4030	ns
	Algae	Sand	12	8	92	0.0002	0.0004	***
	Coral	Sand	14	8	112	0.0000	0.0000	****
Night	Algae	Coral	12	14	91	0.7420	0.7420	ns
	Algae	Sand	12	8	4	0.0002	0.0006	***
	Coral	Sand	14	8	8	0.0004	0.0008	***

Summary of photosynthesis-irradiance curves modelled from coral reef net community production data using the hyperbolic 2 tangent function (Jassby and Platt 1976).

Substrate-specific coefficients for the photosynthesis-irradiance models are displayed with 3 standard error (± SE) and 2.5 % and 97.5 % confidence intervals (CI). The light saturation point (EK) was calculated by dividing 4 maximum gross photosynthesis (Pmax) by alpha (α), the initial slope between NCP and light. Residual Sum of Squares (RSS) and 5 standard area of the regression (σ) calculated to evaluate model fit.

	P_{max}	±SE	CI 2.5%	CI 97.5%	p	α	±SE	CI 2.5%	CI 97.5%	p	E_K	RSS	σ
Algae	11.60	0.86	9.82	13.38	3.96×10^{-12}	0.08	0.01	0.05	0.10	4.08×10^{-06}	151.83	96.98	2.10
Coral	12.08	1.13	9.77	14.40	4.80×10^{-11}	0.08	0.02	0.04	0.11	1.41×10^{-04}	155.07	258.25	3.15
Sand	4.17	0.64	2.79	5.55	1.42×10^{-05}	0.03	0.01	0.01	0.05	9.62×10^{-03}	139.65	24.18	1.31
All	10.13	0.66	8.81	11.45	1.91×10^{-23}	0.07	0.01	0.05	0.08	4.19×10^{-09}	154.62	510.58	2.78

Figure 1

Visual summary of field depployed benthic chambers for case studies 1 and 2.

Photographs depicting: (a) tall version of the chamber constructed using the unchanged plastic bag; (b) low-profile chamber created by cutting the plastic bag into panels and heat sealing in a dome form, for use in high-energy environments; (c) visual assessment of leakage and mixing from the chamber using dispersal of red food dye injected into the chamber; (d) aerial image taken above Akumal Bay showing the sites where chambers were deployed for case studies, photo credit: Edgar Escalante Mancera and Miguel Ángel Gómez Reali; and (e) a schematic diagram of the chamber prototype developed in this study.
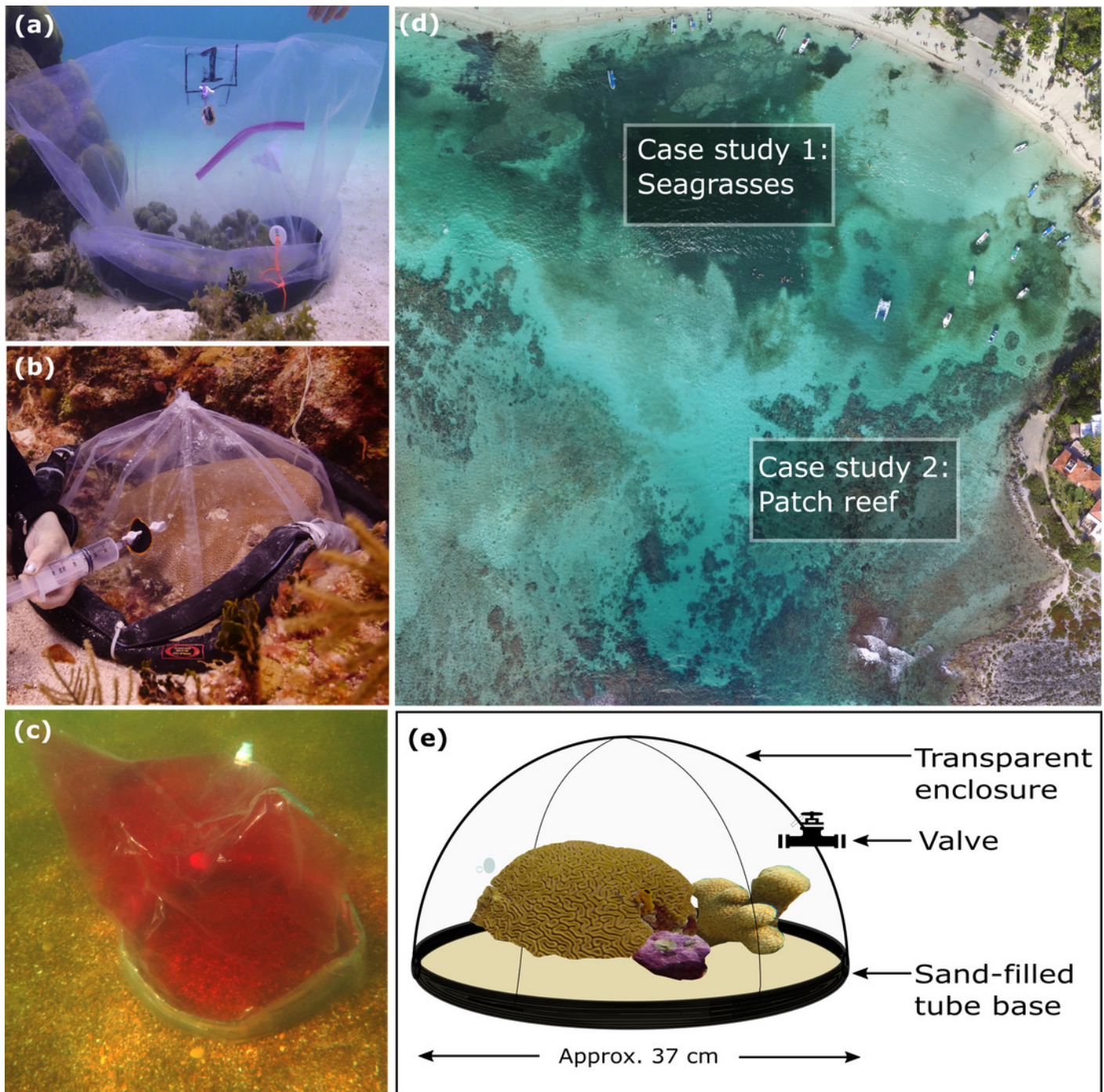
Figure 2

Light transmission of the benthic chamber.

Chamber transparency measured with (a) a spectrophotometer to quantify percentage (%) transmission of light between 400 – 750 nm, and (b) light sensors during the field deployment of chambers (n=3) to measure PAR (μmol m^2 s^{-1}) inside (blue line) and outside (orange dots) of the chamber over 3 days of exposure to natural solar radiation between 07:00 to 19:00 hours.
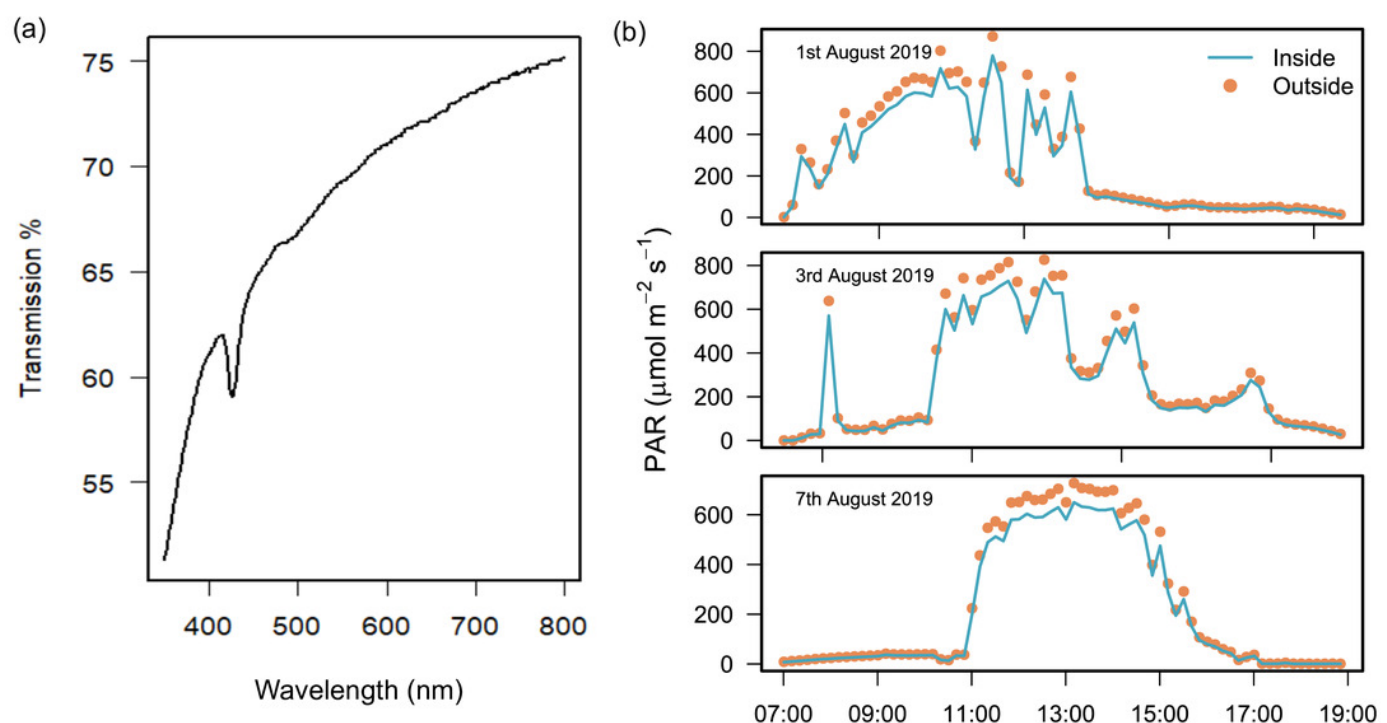
Figure 3

Net community productivity (NCP) of incubated seagrass patches measured from benthic incubations.

NCP was calculated from the change in dissolved oxygen (ΔDO) normalised to chamber volume and incubation time (mmol m^{-2} hr^{-1}). Incubation chambers were deployed simultaneously over seagrasses in the dark (n=5), at solar noon when PAR = mean 757 ±SD 88 μmol m^{-2} s^{-1} (n=6,) and in the late afternoon, PAR = mean 463 ±SD 75 μmol m^{-2} s^{-1} (n=5).
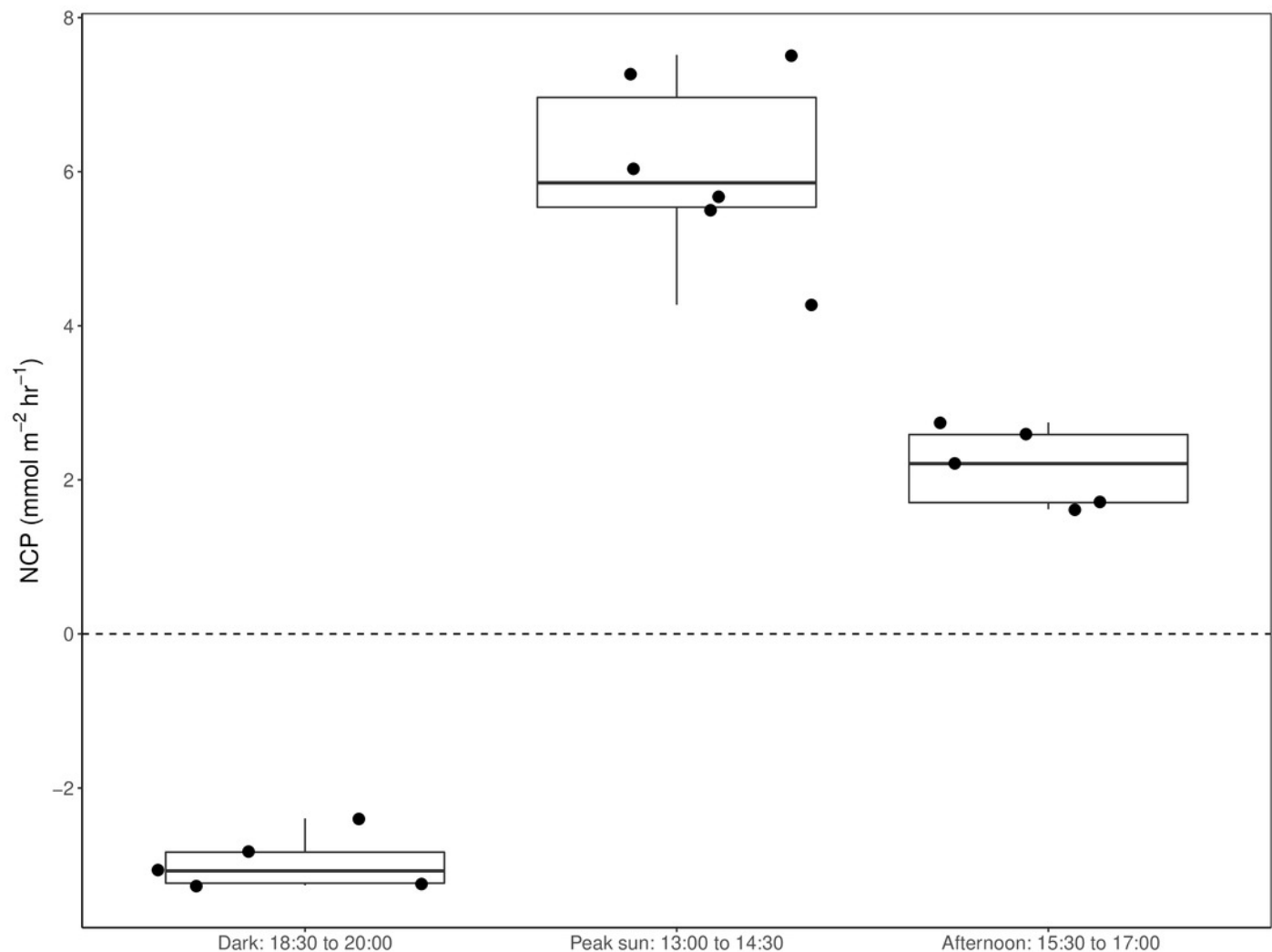
Figure 4

An example of the 3D model generated for each of the incubated patches to measure surface area of complex structures and to estimate the volume occupied by the organism.

3D models were built from photographs taken in-situ to estimate the composition, and measure volume and surface area of each patch: **(a)** screenshot of 3D model built from 85 photographs used for visual assessment of the relative percent cover of coral / algae etc. **(b)** a 3D profile of a coral colony from which volume and surface areas were derived. The surface area of the base of the colony was removed from the overall surface area calculated.
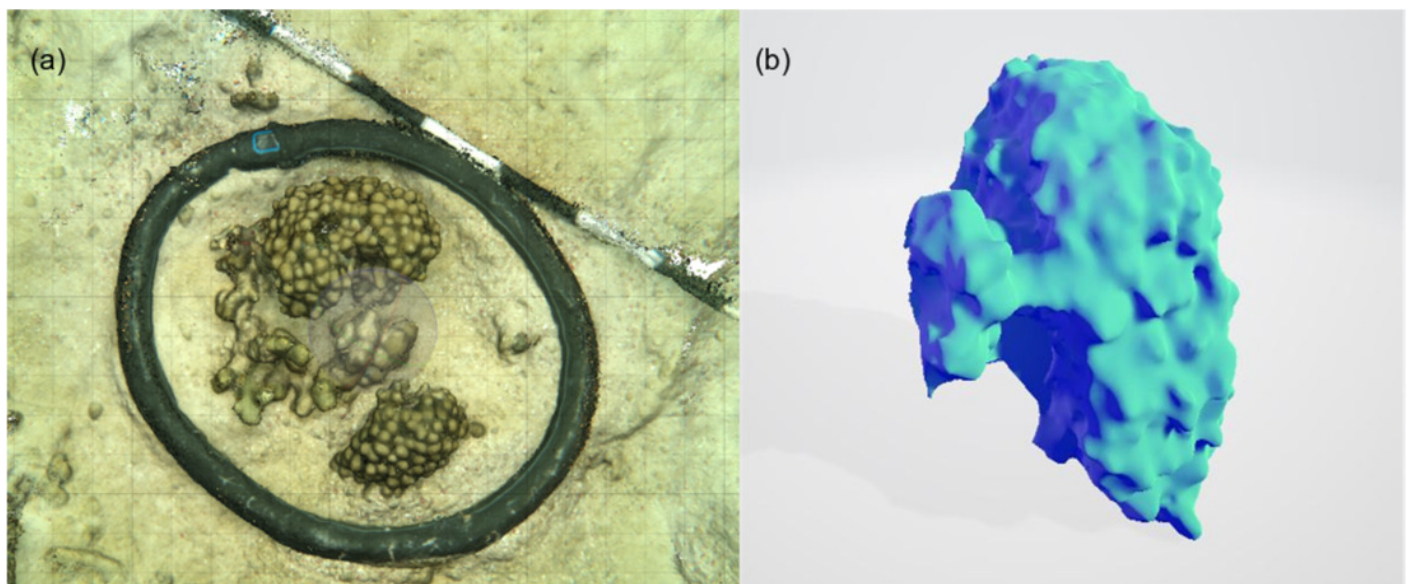
Figure 5

Net community productivity (NCP) per incubated patch over 4 days and nights.

Stacked bar plots (top) show the proportional cover for each category of functional group and the boxplot (bottom) show the rates of NCP (mmol m^{-2} hr^{-1}) measured from differences in dissolved oxygen (ΔDO) normalised to chamber volume and organism surface area (m^2) per hour following equation 1.
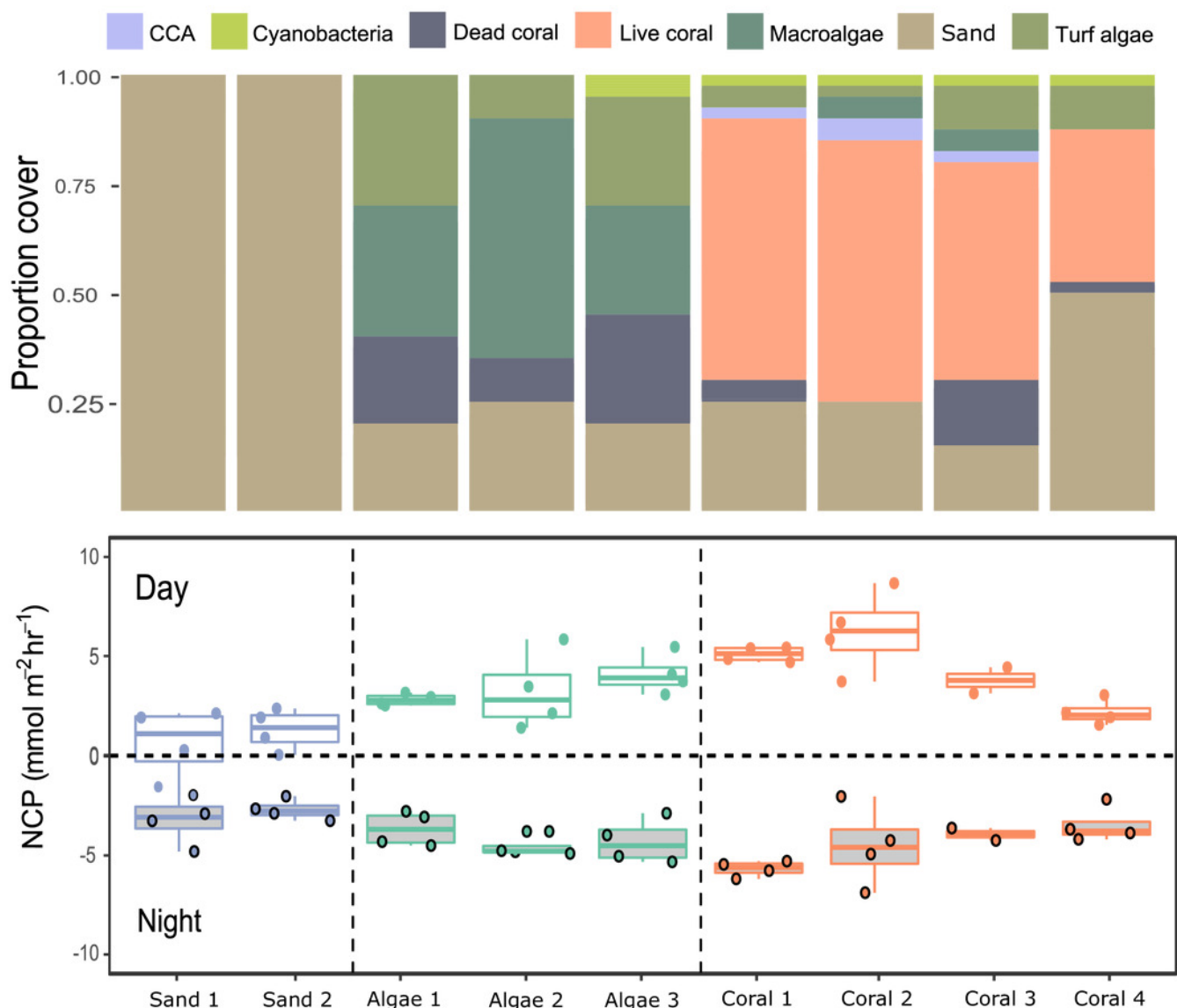
Figure 6

Photosynthesis-irradiance curves fitted for net community production (NCP) of incubated communities of coral-, algae-, and sand-dominated reef patches.

NCP (mmol m-2 hr-1) in relation to PAR (umol photons m^{-2} s^{-1}). Shapes and colours represent the different types of patch incubated. Models were fit by non-linear least squares using the hyperbolic tangent function (Eq.2).